

The Nuclear Force Problem: Is the Never-Ending Story Coming to an End?

R. Machleidt

Department of Physics, University of Idaho, Moscow, Idaho, USA

Abstract. The attempts to find the right (underlying) theory for the nuclear force have a long and stimulating history. Already in 1953, Hans Bethe stated that “more man-hours have been given to this problem than to any other scientific question in the history of mankind”. In search for the nature of the nuclear force, the idea of sub-nuclear particles was created which, eventually, generated the field of particle physics. I will review this productive history of hope, error, and desperation. Finally, I will discuss recent ideas which apply the concept of an effective field theory to low-energy QCD. There are indications that this concept may provide the right framework to properly understand nuclear forces.

1 Historical Perspective

The theory of nuclear forces has a long history (cf. Table 1). Based upon the seminal idea by Yukawa [1], first field-theoretic attempts to derive the nucleon-nucleon (NN) interaction focused on pion-exchange. While the one-pion exchange turned out to be very useful in explaining NN scattering data and the properties of the deuteron [2], multi-pion exchange was beset with serious ambiguities [3, 4]. Thus, the “pion theories” of the 1950s are generally judged as failures – for reasons we understand today: pion dynamics is constrained by chiral symmetry, a crucial point that was unknown in the 1950s.

Historically, the experimental discovery of heavy mesons [5] in the early 1960s saved the situation. The one-boson-exchange (OBE) model [6, 7] emerged which is still the most economical and quantitative phenomenology for describing the nuclear force [8, 9]. The weak point of this model, however, is the scalar-isoscalar “sigma” or “epsilon” boson, for which the empirical evidence remains controversial. Since this boson is associated with the correlated (or resonant) exchange of two pions, a vast theoretical effort that occupied more than a decade was launched to derive the 2π -exchange contribution to the nuclear force, which creates the intermediate range attraction. For this, dispersion theory as well as field theory were invoked producing the Paris [10, 11] and the Bonn [7, 12] potentials.

The nuclear force problem appeared to be solved; however, with the discovery of quantum chromo-dynamics (QCD), all “meson theories” were relegated to models and the attempts to derive the nuclear force started all over again.

The problem with a derivation from QCD is that this theory is non-perturbative in the low-energy regime characteristic of nuclear physics, which makes direct solutions impossible. Therefore, during the first round of new attempts, QCD-inspired

quark models [13] became popular. These models are able to reproduce qualitatively and, in some cases, semi-quantitatively the gross features of the nuclear force [14, 15]. However, on a critical note, it has been pointed out that these quark-based approaches are nothing but another set of models and, thus, do not represent any fundamental progress. Equally well, one may then stay with the simpler and much more quantitative meson models.

A major breakthrough occurred when the concept of an effective field theory (EFT) was introduced and applied to low-energy QCD [16].

Note that the QCD Lagrangian for massless up and down quarks is chirally symmetric, i.e., it is invariant under global flavor $SU(2)_L \times SU(2)_R$ equivalent to $SU(2)_V \times SU(2)_A$ (vector and axial vector) transformations. The axial symmetry is spontaneously broken as evidenced in the absence of parity doublets in the low-mass hadron spectrum. This implies the existence of three massless Goldstone bosons which are identified with the three pions (π^\pm, π^0). The non-zero, but small, pion mass is a consequence of the fact that the up and down quark masses are not exactly zero either (some small, but explicit symmetry breaking). Thus, we arrive at a low-energy scenario that consists of pions and nucleons interacting via a force governed by spontaneously broken approximate chiral symmetry.

To create an effective field theory describing this scenario, one has to write down the most general Lagrangian consistent with the assumed symmetry principles, particularly the (broken) chiral symmetry of QCD [16]. At low energy, the effective degrees of freedom are pions and nucleons rather than quarks and gluons; heavy

Table 1. Seven Decades of Struggle: The Theory of Nuclear Forces

1935	Yukawa: Meson Theory
1950's	<i>The "Pion Theories"</i> One-Pion Exchange: o.k. Multi-Pion Exchange: disaster
1960's	Many pions \equiv multi-pion resonances: $\sigma, \rho, \omega, \dots$ The One-Boson-Exchange Model
1970's	Refine meson theory: Sophisticated 2π exchange models (Stony Brook, Paris, Bonn)
1980's	Nuclear physicists discover QCD Quark Cluster Models
1990's and beyond	Nuclear physicists discover EFT Weinberg, van Kolck Back to Meson Theory! <i>But, with Chiral Symmetry</i>

mesons and nucleon resonances are “integrated out”. So, the circle of history is closing and we are back to Yukawa’s meson theory, except that we have learned to add one important refinement to the theory: broken chiral symmetry is a crucial constraint that generates and controls the dynamics and establishes a clear connection with the underlying theory, QCD.

It is the purpose of the remainder of this paper to describe the EFT approach to nuclear forces in more detail.

2 Chiral Perturbation Theory and the Hierarchy of Nuclear Forces

The chiral effective Lagrangian is given by an infinite series of terms with increasing number of derivatives and/or nucleon fields, with the dependence of each term on the pion field prescribed by the rules of broken chiral symmetry. Applying this Lagrangian to NN scattering generates an unlimited number of Feynman diagrams. However, Weinberg showed [17] that a systematic expansion exists in terms of $(Q/\Lambda_\chi)^\nu$, where Q denotes a momentum or pion mass, $\Lambda_\chi \approx 1$ GeV is the chiral symmetry breaking scale, and $\nu \geq 0$ (cf. Figure 1). This has become known as chiral perturbation theory (χ PT). For a given order ν , the number of terms is finite and calculable; these terms are uniquely defined and the prediction at each order is model-independent. By going to higher orders, the amplitude can be calculated to any desired accuracy.

Following the first initiative by Weinberg [17], pioneering work was performed by Ordóñez, Ray, and van Kolck [18, 19] who constructed a NN potential in coordinate space based upon χ PT at next-to-next-to-leading order (NNLO; $\nu = 3$). The results were encouraging and many researchers became attracted to the new field. Kaiser, Brockmann, and Weise [20] presented the first model-independent prediction for the NN amplitudes of peripheral partial waves at NNLO. Epelbaum *et al.* [21] developed the first momentum-space NN potential at NNLO, and Entem and Machleidt [22] presented the first potential at N³LO ($\nu = 4$).

In χ PT, the NN amplitude is uniquely determined by two classes of contributions: contact terms and pion-exchange diagrams. There are two contacts of order Q^0 [$\mathcal{O}(Q^0)$] represented by the four-nucleon graph with a small-dot vertex shown in the first row of Figure 1. The corresponding graph in the second row, four nucleon legs and a solid square, represent the seven contact terms of $\mathcal{O}(Q^2)$. Finally, at $\mathcal{O}(Q^4)$, we have 15 contact contributions represented by a four-nucleon graph with a solid diamond.

Now, turning to the pion contributions: At leading order [LO, $\mathcal{O}(Q^0)$, $\nu = 0$], there is only the wellknown static one-pion exchange, second diagram in the first row of Figure 1. Two-pion exchange (TPE) starts at next-to-leading order (NLO, $\nu = 2$) and all diagrams of this leading-order two-pion exchange are shown. Further TPE contributions occur in any higher order. Of this sub-leading TPE, we show only two representative diagrams at NNLO and three diagrams at N³LO.

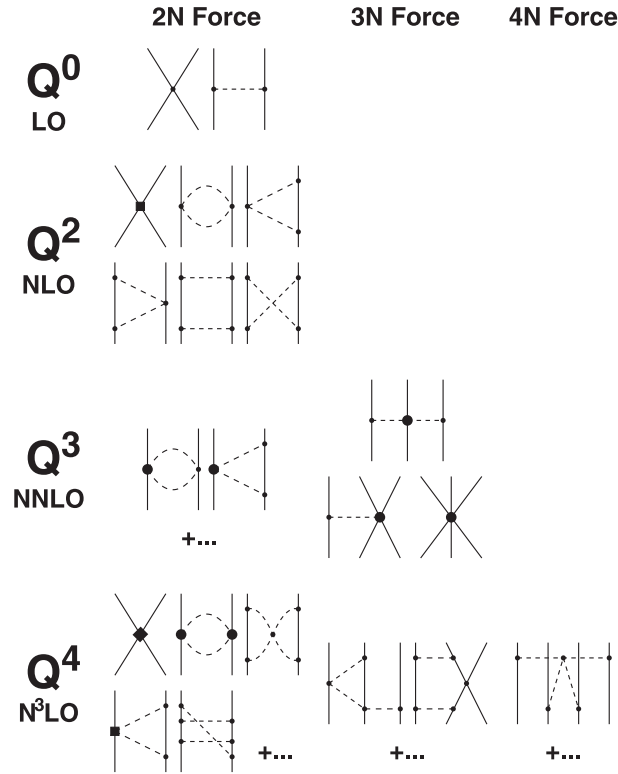


Figure 1. Hierarchy of nuclear forces in χ PT. Solid lines represent nucleons and dashed lines pions. Further explanations are given in the text.

The TPE at N³LO has been calculated first by Kaiser [23]. All 2π exchange diagrams/contributions up to N³LO are summarized in a pedagogical and systematic fashion in [24] where the model-independent results for NN scattering in peripheral partial waves are also shown.

Finally, there is also three-pion exchange, which shows up for the first time at N³LO (two loops; one representative 3π diagram is included in Figure 1). In [25], it was demonstrated that the 3π contribution at this order is negligible.

One important advantage of χ PT is that it makes specific predictions also for many-body forces. For a given order of χ PT, two-nucleon forces (2NF), three-nucleon forces (3NF), ... are generated on the same footing (cf. Figure 1). At LO, there are no 3NF, and at next-to-leading order (NLO), all 3NF terms cancel [17, 26]. However, at NNLO and higher orders, well-defined, nonvanishing 3NF occur [26, 27]. Since 3NF show up for the first time at NNLO, they are weak. Four-nucleon forces (4NF) occur first at N³LO and, therefore, they are even weaker.

3 Chiral NN Potentials

The two-nucleon system is non-perturbative as evidenced by the presence of shallow bound states and large scattering lengths. Weinberg [17] showed that the strong enhancement of the scattering amplitude arises from purely nucleonic intermediate states. He therefore suggested to use perturbation theory to calculate the NN potential and to apply this potential in a scattering equation (Lippmann-Schwinger or Schrödinger equation) to obtain the NN amplitude. We follow this philosophy.

Chiral perturbation theory is a low-momentum expansion. It is valid only for momenta $Q \ll \Lambda_\chi \approx 1$ GeV. Therefore, when a potential is constructed, all expressions (contacts and irreducible pion exchanges) are multiplied with a regulator function,

$$\exp \left[- \left(\frac{p}{\Lambda} \right)^{2n} - \left(\frac{p'}{\Lambda} \right)^{2n} \right], \quad (1)$$

where p and p' denote, respectively, the magnitudes of the initial and final nucleon momenta in the center-of-mass frame; and $\Lambda \ll \Lambda_\chi$. The exponent $2n$ is to be chosen such that the regulator generates powers which are beyond the order at which the calculation is conducted.

NN potentials based upon χ PT at NNLO [21, 28] are poor in quantitative terms; they reproduce the NN data below 290 MeV lab. energy with a χ^2/datum of more than 20 (cf. Tables 2 and 3). As shown first by Entem and Machleidt in 2003 [22], one has to go to order N³LO to obtain a NN potential of acceptable accuracy. For a more recent construction of an N³LO NN potential, see [31].

For an accurate fit of the low-energy pp and np data, charge-dependence is important. Charge-dependence up to next-to-leading order of the isospin-violation scheme (NL \emptyset , in the notation of [32]) includes: the pion mass difference in OPE and the Coulomb potential in pp scattering, which takes care of the L \emptyset contributions. At order NL \emptyset we have pion mass difference in the NLO part of TPE, $\pi\gamma$ exchange [33], and two charge-dependent contact interactions of order Q^0 which make possible an accurate fit of the three different 1S_0 scattering lengths, a_{pp} , a_{nn} , and a_{np} .

Table 2. χ^2/datum for the reproduction of the 1999 np database below 290 MeV by various np potentials. ($\Lambda = 500$ MeV in all chiral potentials.)

Bin (MeV)	# of data	N ³ LO ^a	NNLO ^b	NLO ^b	AV18 ^c
0–100	1058	1.06	1.71	5.20	0.95
100–190	501	1.08	12.9	49.3	1.10
190–290	843	1.15	19.2	68.3	1.11
0–290	2402	1.10	10.1	36.2	1.04

^aReference [22].

^bReference [28].

^cReference [29].

In the optimization procedure, we fit first phase shifts, and then we refine the fit by minimizing the χ^2 obtained from a direct comparison with the data. The χ^2/datum for the fit of the np data below 290 MeV is shown in Table 2, and the corresponding one for pp is given in Table 3. The χ^2 tables show the quantitative improvement of the NN interaction order by order in a dramatic way. Even though there is considerable improvement when going from NLO to NNLO, it is clearly seen that N³LO is needed to achieve an accuracy comparable to the phenomenological high-precision Argonne V_{18} potential [29]. Note that proton-proton data have, in general, smaller errors than np data which explains why the pp χ^2 are always larger.

The phase shifts for np scattering below 300 MeV lab. energy are displayed in Figure 2. What the χ^2 tables revealed, can be seen graphically in this figure. The 3P_2 phase shifts are a particularly good example: NLO (dotted line) is clearly poor. NNLO (dash-dotted line) brings improvement and describes the data up to about 100 MeV. The difference between the NLO and NNLO curves is representative for the uncertainty at NLO and, similarly, the difference between NNLO and N³LO reflects the uncertainty at NNLO. Obviously, at N³LO ($\Lambda = 500$ MeV, thick solid line) we have a good description up to 300 MeV. An idea of the uncertainty at N³LO can be obtained by varying the cutoff parameter Λ . The thick dashed line is N³LO using $\Lambda = 600$ MeV. In most cases, the latter two curves are not distinguishable on the scale of the figures. Noticeable differences occur only in 1D_2 , 3F_2 , and ϵ_2 above 200 MeV.

4 Chiral Three-Nucleon Forces

As noted before, an important advantage of the EFT approach is that it creates two- and many-body forces on an equal footing. The first non-vanishing 3NF terms occur at NNLO and are shown in Figure 1 (row ‘ Q^3/NNLO ’, column ‘3N Force’). There are three diagrams: the TPE, OPE, and 3N-contact interactions [27]. The TPE 3N-potential is given by

Table 3. χ^2/datum for the reproduction of the 1999 pp database below 290 MeV by various pp potentials. ($\Lambda = 500$ MeV in all chiral potentials.)

Bin (MeV)	# of data	N ³ LO ^a	NNLO ^b	NLO ^b	AV18 ^c
0–100	795	1.05	6.66	57.8	0.96
100–190	411	1.50	28.3	62.0	1.31
190–290	851	1.93	66.8	111.6	1.82
0–290	2057	1.50	35.4	80.1	1.38

^aReference [22].

^bSee footnote [30].

^cReference [29].

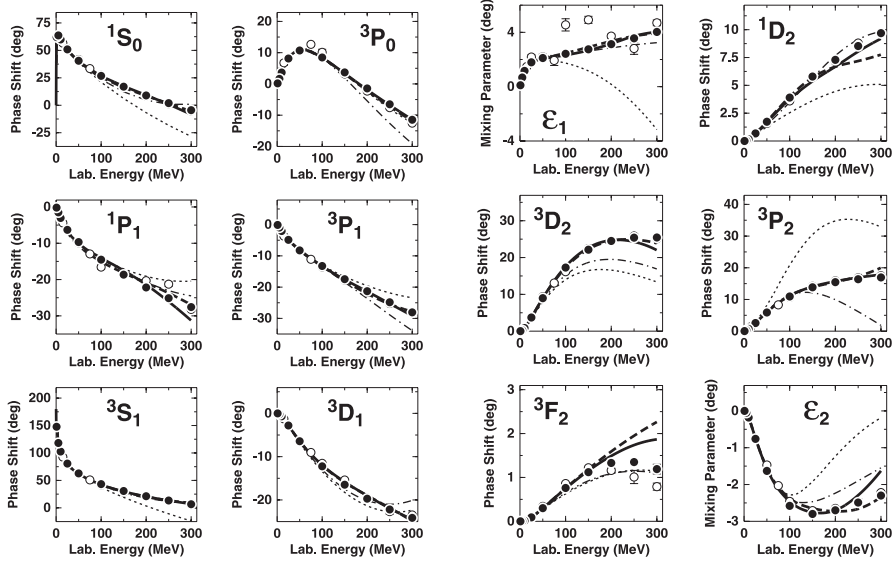


Figure 2. np phase parameters below 300 MeV lab. energy for partial waves with $J \leq 2$. The thick solid (dashed) line is the result by Entem and Machleidt [22] at $N^3\text{LO}$ using $\Lambda = 500$ MeV ($\Lambda = 600$ MeV). The thin dotted and dash-dotted lines are the phase shifts at NLO and NNLO, respectively, as obtained by Epelbaum *et al.* [28] using $\Lambda = 500$ MeV. The solid dots show the Nijmegen multienergy np phase shift analysis [34], and the open circles are the GWU/VPI single-energy np analysis SM99 [35].

$$V_{\text{TPE}}^{3\text{NF}} = \left(\frac{g_A}{2f_\pi}\right)^2 \frac{1}{2} \sum_{i \neq j \neq k} \frac{(\vec{\sigma}_i \cdot \vec{q}_i)(\vec{\sigma}_j \cdot \vec{q}_j)}{(q_i^2 + m_\pi^2)(q_j^2 + m_\pi^2)} F_{ijk}^{\alpha\beta} \tau_i^\alpha \tau_j^\beta \quad (2)$$

with $\vec{q}_i \equiv \vec{p}_i' - \vec{p}_i$, where \vec{p}_i and \vec{p}_i' are the initial and final momenta of nucleon i , respectively, and

$$F_{ijk}^{\alpha\beta} = \delta^{\alpha\beta} \left[-\frac{4c_1 m_\pi^2}{f_\pi^2} + \frac{2c_3}{f_\pi^2} \vec{q}_i \cdot \vec{q}_j \right] + \frac{c_4}{f_\pi^2} \sum_\gamma \epsilon^{\alpha\beta\gamma} \tau_k^\gamma \vec{\sigma}_k \cdot [\vec{q}_i \times \vec{q}_j]. \quad (3)$$

The vertex involved in this 3NF term is the two-derivative $\pi\pi NN$ vertex (large solid dot in Figure 1) which we encountered already in the TPE contribution to the 2N potential at NNLO. Thus, there are no new parameters and the contribution is fixed by the LECs used in NN. The OPE contribution is

$$V_{\text{OPE}}^{3\text{NF}} = D \frac{g_A}{8f_\pi^2} \sum_{i \neq j \neq k} \frac{\vec{\sigma}_j \cdot \vec{q}_j}{q_j^2 + m_\pi^2} (\tau_i \cdot \tau_j) (\vec{\sigma}_i \cdot \vec{q}_j) \quad (4)$$

and, finally, the 3N contact term reads

$$V_{\text{ct}}^{3\text{NF}} = E \frac{1}{2} \sum_{j \neq k} \tau_j \cdot \tau_k. \quad (5)$$

The last two 3NF terms involve two new vertices (that do not occur in the 2N problem), namely, the $\pi NNNN$ vertex with parameter D and a $6N$ vertex with parameters E . One way to pin down the two new parameters is to fit them to the triton and the ${}^4\text{He}$ binding energies. Once D and E are fixed, the results for other 3N, 4N, ... observables are predictions. Results for 3N scattering observables are reported in [36, 37]. Spectra of light nuclei are calculated in [38, 39]. Concerning the famous ‘ A_y puzzle’, the above 3NF terms yield some improvement of the predicted nucleon-deuteron analyzing powers, however, the problem is not resolved.

One should note that there are additional 3NF terms at NNLO due to relativistic corrections ($1/M_N$ corrections) that have not yet been included in any calculation. However, there are all reasons to believe that these contributions will be very small, probably negligible. It is more likely that the problem with the chiral 3NF is analogous to the one with the chiral 2NF: namely, NNLO is insufficient and for sufficient accuracy one has to proceed to $N^3\text{LO}$. Two 3NF topologies at $N^3\text{LO}$ are indicated in Figure 1. The $N^3\text{LO}$ 3NF, which does not depend on any new parameters, is presently under development.

5 Conclusions

The EFT approach to nuclear forces is a modern refinement of Yukawa’s meson theory. It represents a scheme that has an intimate relationship with QCD and allows to calculate nuclear forces to any desired accuracy. Moreover, nuclear two- and many-body forces are generated on the same footing.

At $N^3\text{LO}$ [22], the accuracy is achieved that is necessary and sufficient for microscopic nuclear structure. First calculations applying the $N^3\text{LO}$ NN potential in the no-core shell model [40–42], the coupled cluster formalism [43–48], and the unitary-model-operator approach [49] have produced promising results.

The 3NF at NNLO is known [27] and has had first successful applications in few-nucleon reactions [36, 37] as well as the structure of light nuclei [38, 39]. The 3NF at $N^3\text{LO}$ is under construction.

It may be too early to claim that the never-ending story is coming to an end, but the story is certainly converging.

Acknowledgments

This work was supported in part by the U.S. National Science Foundation under Grant No. PHY-0099444.

References

1. H. Yukawa, *Proc. Phys. Math. Soc. Japan* **17**, 48 (1935).
2. *Prog. Theor. Phys. (Kyoto) Supplement* **3**, (1956).

3. M. Taketani *et al.*, *Prog. Theor. Phys. (Kyoto)* **7**, 45 (1952).
4. K.A. Brueckner *et al.*, *Phys. Rev.* **90**, 699 (1953); *ibid.* **92**, 1023 (1953).
5. A.R. Erwin *et al.*, *Phys. Rev. Lett.* **6**, 628 (1961); B.C. Maglič *et al.*, *Phys. Rev. Lett.* **7**, 178 (1961).
6. *Prog. Theor. Phys. (Kyoto) Supplement* **39**, (1967); R.A. Bryan and B.L. Scott, *Phys. Rev.* **177**, 1435 (1969); M.M. Nagels *et al.*, *Phys. Rev. D* **17**, 768 (1978).
7. R. Machleidt, *Adv. Nucl. Phys.* **19**, 189 (1989).
8. V.G.J. Stoks *et al.*, *Phys. Rev. C* **49**, 2950 (1994).
9. R. Machleidt, *Phys. Rev. C* **63**, 024001 (2001).
10. R. Vinh Mau, *Mesons in Nuclei*, Vol. I, ed M. Rho and D.H. Wilkinson (North-Holland, Amsterdam) p. 151 (1979).
11. M. Lacombe *et al.*, *Phys. Rev. C* **21**, 861 (1980).
12. R. Machleidt *et al.*, *Phys. Rep.* **149**, 1 (1987).
13. F. Myhrer *et al.*, *Rev. Mod. Phys.* **60**, 629 (1988).
14. D.R. Entem, F. Fernandez, and A. Valcarce, *Phys. Rev. C* **62**, 034002 (2000).
15. G.H. Wu, J.L. Ping, L.J. Teng, F. Wang, and T. Goldman, *Nucl. Phys. A* **673**, 273 (2000).
16. S. Weinberg, *Physica* **96A**, 327 (1979).
17. S. Weinberg, *Nucl. Phys. B* **363**, 3 (1991).
18. C. Ordóñez, L. Ray, and U. van Kolck, *Phys. Rev. C* **53**, 2086 (1996).
19. U. van Kolck, *Prog. Part. Nucl. Phys.* **43**, 337 (1999).
20. N. Kaiser *et al.*, *Nucl. Phys. A* **625**, 758 (1997).
21. E. Epelbaum *et al.*, *Nucl. Phys. A* **671**, 295 (2000).
22. D.R. Entem and R. Machleidt, *Phys. Rev. C* **68**, 041001 (2003).
23. N. Kaiser, *Phys. Rev. C* **64**, 057001 (2001); *ibid.* **65** 017001 (2001).
24. D.R. Entem and R. Machleidt, *Phys. Rev. C* **66**, 014002 (2002).
25. N. Kaiser, *Phys. Rev. C* **61**, 014003 (1999); *ibid.* **62** 024001 (1999).
26. U. van Kolck, *Phys. Rev. C* **49**, 2932 (1994).
27. E. Epelbaum *et al.*, *Phys. Rev. C* **66**, 064001 (2002).
28. E. Epelbaum *et al.*, *Eur. Phys. J. A* **15**, 543 (2002).
29. R.B. Wiringa, V.G.J. Stoks, and R. Schiavilla, *Phys. Rev. C* **51**, 38 (1995).
30. Since [28] provides only the np versions of the NLO and NNLO potentials, we have constructed the pp versions by incorporating charge-dependence and minimizing the pp χ^2 .
31. E. Epelbaum, W. Glöckle, and U.G. Meissner, *Nucl. Phys. A* **747**, 362 (2005).
32. M. Walzl *et al.*, *Nucl. Phys. A* **693**, 663 (2001).
33. U. van Kolck *et al.*, *Phys. Rev. Lett.* **80**, 4386 (1998).
34. V.G.J. Stoks, R.A.M. Klomp, M.C.M. Rentmeester, and J.J. de Swart, *Phys. Rev. C* **48**, 792 (1993).
35. R.A. Arndt, I.I. Strakowsky, and R.L. Workman, George Washington University Data Analysis Center (formerly VPI SAID facility), solution of summer 1999 (SM99), (1999).
36. K. Ermisch *et al.*, *Phys. Rev. C* **71**, 064004 (2005).
37. H. Witala, J. Golak, R. Skibinski, W. Glöckle, A. Nogga, E. Epelbaum, H. Kamada, A. Kievsky, and M. Viviani *Phys. Rev. C* **73**, 044004 (2006).
38. A. Nogga *et al.*, *Nucl. Phys. A* **737**, 236 (2004).
39. A. Nogga, P. Navrátil, B.R. Barrett, and J.P. Vary, *Phys. Rev. C* **73**, 064002 (2006).
40. P. Navrátil and E. Caurier, *Phys. Rev. C* **69**, 014311 (2004).
41. C. Forssen, P. Navrátil, W.E. Ormand, and E. Caurier, *Phys. Rev. C* **71**, 044312 (2005).
42. J.P. Vary *et al.*, *Eur. Phys. J. A* **25** s01, 475 (2005).
43. K. Kowalski, D.J. Dean, M. Hjorth-Jensen, and T. Papenbrock, *Phys. Rev. Lett.* **92**, 132501 (2004).

44. D.J. Dean and M. Hjorth-Jensen, *Phys. Rev. C* **69**, 054320 (2004).
45. M. Wloch *et al.*, *J. Phys. G* **31**, S1291 (2005).
46. M. Wloch *et al.*, *Phys. Rev. Lett.* **94**, 21250 (2005).
47. D.J. Dean *et al.*, *Nucl. Phys.* **752**, 299 (2005).
48. J.R. Gour *et al.*, *Phys. Rev. C* **74**, 024310 (2006).
49. S. Fujii, R. Okamoto, and K. Suzuki, *Phys. Rev. C* **69**, 034328 (2004).